



Theoretical Evaluation of Some Compounds with Antifungal Effect as Corrosion Inhibitors for Copper in Nitric Acid Solution: DFT Calculations

Cissé M'Bouillé ^a, Mougo André Tigori ^{a*}, Mohamadou Lamine Doumbia ^a,
Paulin Marius Niamien ^b, Mohamed Ebn Touhami ^c and Mouhcine Sfaira ^d

^a *Laboratoire des Sciences et Technologies de l'Environnement, UFR Environnement, Université Jean Lorougnon Guédé, BP 150 Daloa, Côte d'Ivoire.*

^b *Laboratoire de Constitution et de Réaction de la Matière, UFR SSMT, Université Félix Houphouët-Boigny, 22 BP 582 Abidjan 22, Côte d'Ivoire.*

^c *Laboratoire d'Ingénierie des Matériaux et Environnement: Modélisation et Application, Faculté des Sciences, Université Ibn Tofaïl, BP. 133-14000 Kénitra, Morocco.*

^d *Mouhcine Sfaira, Laboratoire d'Ingénierie des Matériaux, de Modélisation et d'Environnement, Faculté des Sciences Dhar El Mahraz, Université Sidi Mohammed Ben Abdellah, BP 1796-30000 Fès, Atlas, Morocco.*

Authors' contributions

This work was carried out in collaboration among all authors. All authors read and approved the final manuscript.

Article Information

DOI: 10.9734/IRJPAC/2022/v23i130448

Open Peer Review History:

This journal follows the Advanced Open Peer Review policy. Identity of the Reviewers, Editor(s) and additional Reviewers, peer review comments, different versions of the manuscript, comments of the editors, etc are available here: <https://www.sdiarticle5.com/review-history/85376>

Original Research Article

Received 20 February 2022

Accepted 26 March 2022

Published 02 April 2022

ABSTRACT

Quantum chemical calculations based on Density Functional Theory (DFT) at the B3LYP/6-31G (d,p) basis set were used to study the inhibition performance of four antifungal organic molecules in copper corrosion in 1M nitric acid solution. The quantum chemical descriptors analysis shows that the investigated compounds have good inhibitory abilities in combating copper corrosion. It results that the inhibition efficiency of these molecules is a function of highest occupied molecular orbital (HOMO), lowest unoccupied molecular orbital (LUMO) and the energy gap. The inhibition performance of these molecules increases when the energy gap decreases. Finally, the areas containing N, S and C atoms are the most likely sites to bind to the copper surface either by donating or receiving electrons.

*Corresponding author: E-mail: tigori20@yahoo.fr;

Keywords: *Quantum chemical calculations; density functional theory; inhibition performance; antifungal; copper corrosion.*

1. INTRODUCTION

The degradation of materials and their physical-chemical properties due to corrosion is a detrimental process that causes huge economic losses and has led to many studies and researches. These various researchers have found suitable organic corrosion inhibitors in various corrosive media [1-3]. Sometimes these research studies are often based on experimentation. Although experimental studies are simple, they are often tedious, time consuming and expensive. Continued advances in hardware and software have opened the door to powerful use of theoretical chemistry in the search for corrosion inhibitors. Several quantum chemical methods and molecular modeling techniques have been used to correlate the inhibitors inhibition efficiency with their molecular properties [4-8]. The theoretical parameters use permits the characterization of the molecular inhibitors structure and proposes their mechanism of interaction with metal surfaces [9,10]. Advances in methodology and implementations have reached a point where predicted properties with reasonable accuracy can be obtained from density functional theory (DFT) calculations. Density functional theory is based on the postulate proposed by Thomas [11] and Fermi [12] that electronic properties can be described in terms of electron density functional. In this theory the multi-electron wave function is replaced by the electron density as the basic quantity for the calculations. The methods for solving the Hartree-Fock and DFT calculations are very similar, and therefore require comparable resources. However the correlation is included in the DFT, so the results are better for similar computation times. Some research in this area has proven that the protective activity of an inhibitor generally depends on several physicochemical and electronic properties of the protective molecules, in particular, its organic functional groups, steric properties, electron density of the contributing atoms, and the orbital characteristic of the electron sharing [13-15]. Indeed, a number of these inhibitors are also highly hazardous to health and the environment, and are the subject of increasing ecological scrutiny and strict environmental regulations. Current research efforts are now focusing on development of non-toxic, low-cost and environmentally friendly corrosion inhibitors as alternatives [16,17]. The electronic structural

features required for corrosion inhibitors, such as the presence of heteroatoms, extensive conjugation, and substituted heterocycles, are readily found in biochemical compounds used as drugs [18-22]. Interestingly, some drugs have been shown to be effective in inhibiting certain metals. In order to comply with the recommendations on the preservation of the environment and to promote the health of all, this work has focused on studying the inhibitory power of four therapeutic molecules with an antifungal effect (Fig. 1), which are ketoconazole, clotrimazole, thiabendazole and tioconazole for copper corrosion in acidic medium. These drugs were chosen because they would not be toxic and they all contain the heteroatoms oxygen (O), nitrogen (N) and sulfur (S) which are at the heart of the electronic exchanges between the metal and these molecules. The reactive capacity of the inhibitor is closely related to its frontier molecular orbital (FMO), including the highest occupied molecular orbital, HOMO, and the lowest unoccupied molecular orbital, LUMO, as well as other parameters such as the energy gap and the fraction of transferred electrons.

The aim of this study is to theoretically investigate the anticorrosive properties of the four antifungals mentioned above and to propose a mechanism of inhibition of the compounds for copper corrosion in nitric acid medium. This research will help to understand the essential elements of a molecule that are involved in the inhibition process.

Quantum chemistry calculations based essentially on Density Functional Theory (DFT) were used in this study to explain how these molecules will be able to protect copper in an acidic environment.

2. METHODS

2.1 Theoretical Calculations Details

In this work, theoretical calculations are based on Density Functional Theory (DFT). All calculations in the gas and aqueous phases were performed using the Gaussian 09 software suite [23]. The geometry optimizations were carried out using the hybrid functional B3LYP (Beckes three-parameter with Lee–Yang–Parr) with 6-31G (d) basis set [24,25].

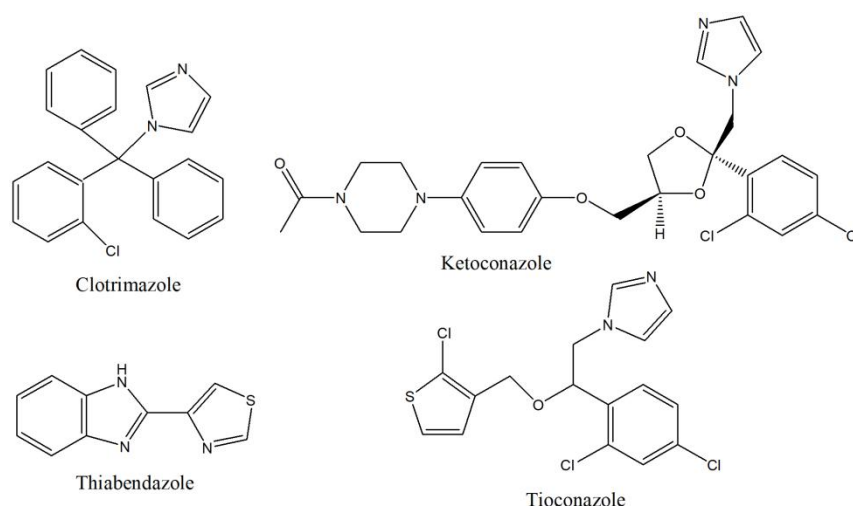


Fig. 1. The molecular structures of the investigated inhibitors

Moreover the quantum chemical parameters such as as highest occupied molecular orbital energy (E_{HOMO}), lowest unoccupied molecular orbital energy (E_{LUMO}), energy gap (ΔE), ionization potential (I), electron affinity (A) dipole moment (μ), electronegativity χ , hardness η , softness S , electrophilicity index ω , Fukui function f_k^+ or f_k^- and dual descriptor ($\Delta f_k(r)$).

The energy gap is determined by the following expression:

$$\Delta E = E_{LUMO} - E_{HOMO} \quad (1)$$

The ionization potential (I) and electron affinity (A) of the inhibitors are calculated according to Koopman's theorem [26]

$$I = -E_{HOMO} \quad (2)$$

$$A = -E_{LUMO} \quad (3)$$

The electronegativity (χ) [27] and the hardness (η) [28] of the inhibitors were estimated using the value of I and A that given by:

$$\chi = -\mu_p = \left(\frac{\partial E}{\partial N}\right)_{v(r)} \quad (4)$$

$$\chi = \frac{I+A}{2} \quad (5)$$

$$\eta = \frac{I-A}{2} \quad (6)$$

The global softness (S) is obtained from the equation [28]:

$$S = \frac{1}{\eta} = \frac{2}{I-A} \quad (7)$$

The global electrophilicity index (ω) [29] is defined as follows:

$$\omega = \frac{(I+A)^2}{4(I-A)} \quad (8)$$

The fraction of electrons transferred (ΔN) from the inhibitor molecule to the metal was performed according to Pearson's electronegativity relationship [30]:

$$\Delta N = \frac{\chi_{Cu} - \chi_{inh}}{2(\eta_{Cu} + \eta_{inh})} \quad (9)$$

where χ_{Cu} and η_{Cu} , χ_{inh} and η_{inh} denote the electronegativity and hardness of copper and the inhibitor molecule respectively. In our case we use the theoretical value of $\chi_{Cu} = 4.98$ eV/mol and $\eta_{Cu} = 0$ [31] assuming that for a metallic charge $I = A$ [32], for the calculation of the number of transferred electrons.

In order to locate the sites of reactivity within each molecule, the Fukui functions were determined from Mulliken charges. Fukui functions, which can be determined using the finite difference approximation:

$$\text{Nucleophilic attack } f_k^+ = q_k(N+1) - q_k(N) \quad (13)$$

$$\text{Electrophilic attack } f_k^- = q_k(N) - q_k(N-1) \quad (14)$$

Where $q_k(N + 1)$, $q_k(N)$ and $q_k(N - 1)$ are the electronic population of atom k in $(N + 1)$, N and $(N - 1)$ electrons systems.

The dual descriptor was introduced to unambiguously explain the sites of local reactivity [33,34]. This descriptor can be determined by the following relations:

$$\Delta f_k(r) = \left(\frac{\partial f_k(r)}{\partial N} \right)_{v(r)} \quad (15)$$

$$\Delta f_k(r) = f_k^+ - f_k^- \quad (16)$$

3. RESULTS AND DISCUSSION

3.1 Molecules optimized forms

The optimized structures of the studied molecules performed by DFT with labels by B3LYP/6-31G (d) are represented by the Fig. 2.

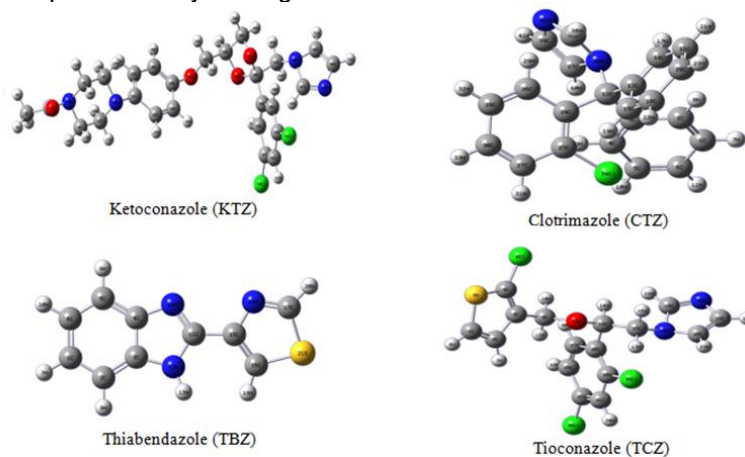


Fig. 2. Optimized structure of KTZ, CTZ, TBZ and TCZ calculated with B3LYP/6-31G (d)

Table 1. Quantum chemical parameters of the studied compounds calculated using B3LYP/6-31G (d)

Parameters	Ketoconazole	Clotrimazole	Thiabendazole	Tioconazole
E_{HOMO} (eV)	-5.5553	-5.9233	-5.8341	-6.1246
E_{LUMO} (eV)	-0.9365	-0.7115	-1.3410	-1.1788
Energy gap ΔE (eV)	4.6188	5.2118	4.4931	4.9458
Dipole moment μ (D)	6.0900	2.3297	3.4576	3.3014
Ionization energy I (eV)	5.5553	5.9233	5.8341	6.1246
Electron affinity A (eV)	0.9365	0.7115	1.3410	1.1788
Electronegativity χ (eV)	3.2459	3.3174	3.5875	3.6517
Hardness η (eV)	2.3094	2.6059	2.2466	2.4728
Softness S (eV) ⁻¹	0.4330	0.3837	0.4451	0.4043
Fraction of electron transferred ΔN	0.3754	0.3190	0.3099	0.2685
Electrophilicity index ω	2.2810	2.1113	2.8644	2.6962
Total energy E_T (Ha)	-2447.7078	-1417.9664	-947.6897	-2580.8709

3.2 Global Reactivity Parameters Analysis

The values of the calculated quantum chemical global parameters with the B3LYP/6-31G (d) are listed in Table 1.

According the molecular orbitals theory, chemical reactivity is a function of the interaction between the HOMO and LUMO levels of the reacting species [35]. E_{HOMO} is a quantum chemical parameter which indicates that a molecule can give electrons to a suitable acceptor system of low energy molecular orbital empty [36]. The analysis of the values obtained show that Ketoconazole has the highest value of E_{HOMO} , however it could have the best ability to donate electrons to the metal.

These molecules do not only supply electrons to the «d» orbitals of metal ions such as Cu^{2+} ([Ar] $3d^9$), but they can also receive electrons from

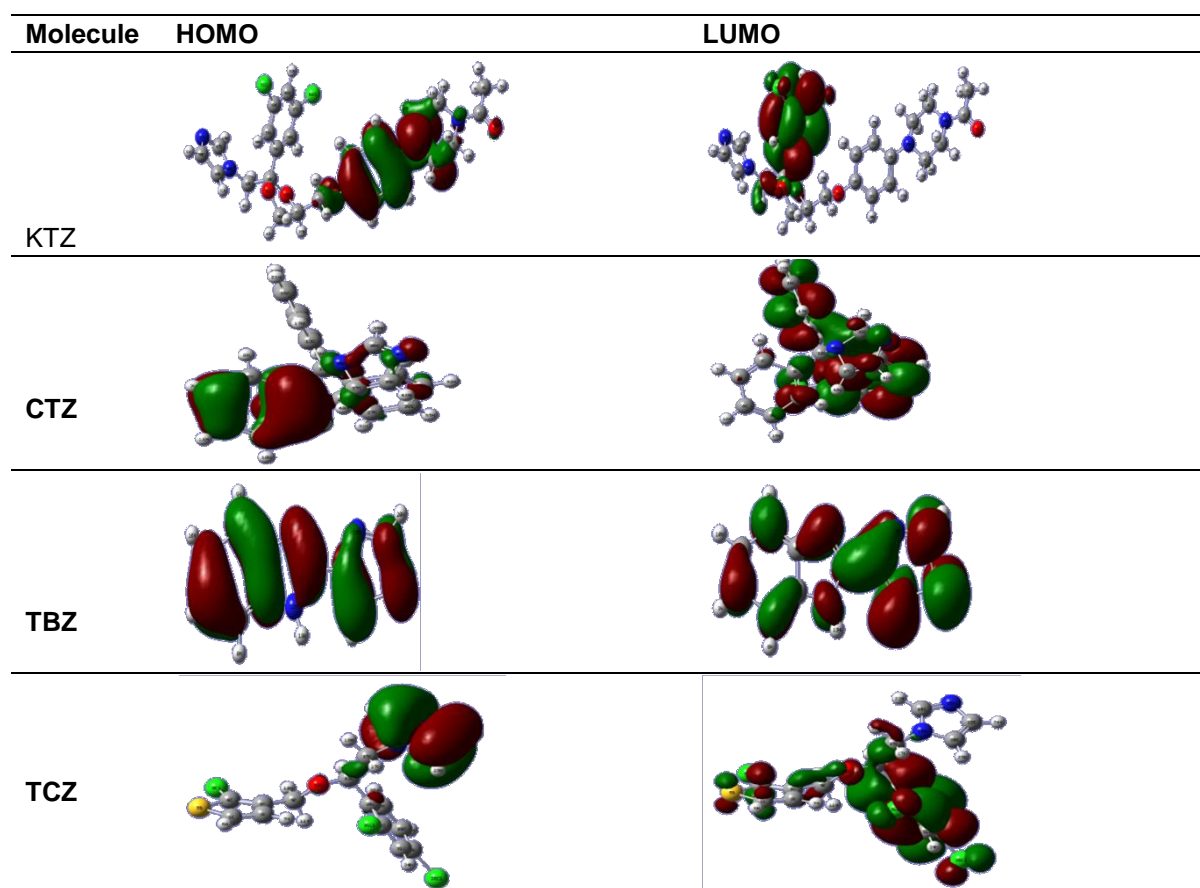


Fig. 3. HOMO and LUMO orbitals of KTZ, CTZ, TBZ and TCZ using DFT at B3LYP/6-31G (d)

these «d» orbitals, leading to a mutual exchange of electrons [37]. In our case, the low E_{LUMO} values show that these molecules tend to receive electrons. The lower the values of E_{LUMO} , the more probable it is that the molecules accept electrons. The binding capacity of the inhibitor to the metal surface increases with increasing HOMO and decreasing LUMO energy values because the geometry of the inhibitor's base state and the nature of its frontier molecular orbitals, HOMO and LUMO, are involved in the inhibition process [37,38]. It should be noted that the electron density of HOMO location in each molecule is mainly distributed near the nitrogen (N) and oxygen (O) atoms showing that these are the preferred sites for adsorption, whereas the LUMO density was distributed almost of the entire molecules. The HOMO-LUMO diagrams of the molecules are shown in Fig. 3.

By analyzing the HOMO–LUMO energy gap values for these molecular compounds in Table 1, it can be noted that TBZ has the lowest energy gap value. Therefore this compound can be predicted to be best corrosion inhibitor compared

to other molecules studied. Indeed when the value of ΔE is low, the electronic transfer between HOMO and LUMO orbitals is easier [39,40]. This good inhibition performance that TBZ could possess is due to the presence of heteroatoms (N, S) and π bonds able to ensure a good interaction between the metal and the molecules.

According to the literature [18,19] there is no consensus on the correlation between the dipole moment (μ) and the inhibition efficiency of an organic.

Referring to the table, all the molecules studied have a low electronegativity value compared to that of copper ($\chi_{Cu}=4.98$ eV). In this case the movement of electrons will be from each molecule to the metal. It appears therefore that the ability of these molecules to protect copper against corrosion will be by receiving their electrons. In fact, the electron flow will happen from the system with the low electronegativity towards that of a higher value until the chemical potentials are the same [30].

We can observe from Table 1 that the hardness (η) values of the studied compounds are in the following order: $\eta(\text{TBZ}) < \eta(\text{KTZ}) < \eta(\text{TCZ}) < \eta(\text{CTZ})$. This order is the reverse of that obtained for global softness. Thus, the inhibitor with the least value of global hardness (hence the highest value of global softness) could have the best inhibition performance in controlling copper corrosion in acidic media. In this case TBZ could protect the copper better against corrosion than the other compounds studied

The fraction of electrons transferred (ΔN) values of the studied compounds are lower than 3.6. It follows in this case that these compounds give electrons to copper in order to strengthen its surface [41]. In fact during the copper corrosion, it loses electrons. In order to protect it, each compound will give electrons to compensate for the lost electrons.

The studied molecules can be good inhibitors for copper corrosion because on the one hand the unoccupied d orbitals of Cu^{2+} ($[\text{Ar}]3d^9$) can

accept electrons from the inhibitors to form a coordination bond. On the other hand, the inhibitor molecules can also accept electrons from the Cu^{2+} ions with a coordination bond. These donation and back donation processes strengthen the adsorption of the inhibitors molecules onto copper surface.

The total energy values are all negative, this implies that the transfer of electrons metal-molecule is possible [42,43].

3.3 Local Reactivity Parameters Analysis

In order to locate the sites capable of donating or accepting electrons Mulliken charges and Fukui indices of each molecule were calculated [44-47]. In addition, the dual descriptors were also determined to unambiguously locate the active sites of the inhibitor molecules. The results are grouped in Tables 2,3,4 and 5. The analysis of these results will allow to understand the interactions of each inhibitor with the metal.

Table 2. Mulliken atomic charges, Fukui indices and dual descriptor of KTZ using DFT at B3LYP/6-31G (d)

Atoms	$q_k(N+1)$	$q_k(N)$	$q_k(N-1)$	f_k^+	f_k^-	$\Delta f_k(r)$
1 C	-0.008043	0.575909	0.012710	-0.583952	0.563199	-1.147151
2 O	0.017543	-0.506838	0.004915	0.524381	-0.511753	1.036134
3 C	0.000552	-0.549299	-0.001201	0.549851	-0.548098	1.097949
4 H	-0.000195	0.168155	0.000925	-0.168350	0.167230	-0.335580
5 H	-0.000071	0.189323	0.000032	-0.189394	0.189291	-0.378685
6 H	-0.000277	0.167769	0.001297	-0.168046	0.166472	-0.334518
7 C	0.006127	-0.144312	-0.000291	0.150439	-0.144021	0.294460
8 C	-0.000231	-0.141538	-0.000040	0.141307	-0.141498	0.282805
9 C	-0.015238	-0.136170	0.000744	0.120932	-0.136914	0.257846
10 H	0.004257	0.148743	0.001154	-0.144486	0.147589	-0.292075
11 H	-0.000050	0.194712	-0.000051	-0.194762	0.194763	-0.389525
12 C	-0.009774	-0.132965	0.001238	0.123191	-0.134203	0.257394
13 H	0.005975	0.152318	0.000546	-0.146343	0.151772	-0.298115
14 H	-0.000474	0.159486	0.000001	-0.159960	0.159485	-0.319445
15 H	0.001118	0.156714	0.002786	-0.155596	0.153928	-0.309524
16 H	0.027730	0.134635	-0.000200	-0.106905	0.134835	-0.241740
17 H	0.000584	0.156685	0.002371	-0.156101	0.154314	-0.310415
18 H	0.031058	0.134527	-0.000409	-0.103469	0.134936	-0.238405
19 N	0.030384	-0.423317	-0.000891	0.453701	-0.422426	0.876127
20 N	0.310112	-0.503597	-0.000757	0.813709	-0.502840	1.316549
21 C	0.043237	0.328785	-0.024233	-0.285548	0.353018	-0.638566
22 C	0.079125	-0.178086	0.094625	0.257211	-0.272711	0.529922
23 C	0.072460	-0.195317	0.059622	0.267777	-0.254939	0.522716
24 C	-0.037948	-0.173642	0.071123	0.135694	-0.244765	0.380459
25 H	-0.003578	0.134319	-0.005516	-0.137897	0.139835	-0.277732
26 C	-0.017413	-0.177690	0.092555	0.160277	-0.270245	0.430522

Atoms	$q_k(N+1)$	$q_k(N)$	$q_k(N-1)$	f_k^+	f_k^-	$\Delta f_k(r)$
27 H	-0.003641	0.135763	-0.003699	-0.139404	0.139462	-0.278866
28 C	0.144381	0.352328	-0.026517	-0.207947	0.378845	-0.586792
29 H	0.001074	0.145943	-0.001707	-0.144869	0.147650	-0.292519
30 H	0.000622	0.133315	-0.005546	-0.132693	0.138861	-0.271554
31 O	0.028580	-0.543523	0.000202	0.572103	-0.543725	1.115828
32 C	0.003871	-0.025738	0.000775	0.029609	-0.026513	0.056122
33 H	-0.000161	0.151449	0.001444	-0.151610	0.150005	-0.301615
34 H	0.002836	0.131351	-0.000184	-0.128515	0.131535	-0.260050
35 C	0.000430	0.087967	-0.000718	-0.087537	0.088685	-0.176222
36 C	0.000090	-0.062528	0.000519	0.062618	-0.063047	0.125665
37 H	-0.000042	0.163990	0.000763	-0.164032	0.163227	-0.327259
38 C	0.000266	0.468778	-0.000061	-0.468512	0.468839	-0.937351
39 H	0.000112	0.167708	0.000242	-0.167596	0.167466	-0.335062
40 H	0.000550	0.150445	0.000446	-0.149895	0.149999	-0.299894
41 O	0.002972	-0.510863	0.003940	0.513835	-0.514803	1.028638
42 O	0.000037	-0.513438	0.003260	0.513475	-0.516698	1.030173
43 C	-0.000042	-0.158424	0.014025	0.158382	-0.172449	0.330831
44 H	-0.000086	0.178099	-0.000676	-0.178185	0.178775	-0.356960
45 H	0.000174	0.168733	0.010427	-0.168559	0.158306	-0.326865
46 N	-0.013430	-0.373661	-0.001262	0.360231	-0.372399	0.732630
47 C	0.114900	0.198498	0.000291	-0.083598	0.198207	-0.281805
48 C	0.125796	0.004832	0.000153	0.120964	0.004679	0.116285
49 H	-0.005636	0.154261	-0.000093	-0.159897	0.154354	-0.314251
50 C	0.091436	-0.037201	0.000068	0.128637	-0.037269	0.165906
51 H	-0.005351	0.156774	0.000035	-0.162125	0.156739	-0.318864
52 H	-0.004638	0.135526	0.000014	-0.140164	0.135512	-0.275676
53 N	-0.024581	-0.435374	0.000582	0.410793	-0.435956	0.846749
54 C	0.000418	0.089263	0.283483	-0.088845	-0.194220	0.105375
55 C	-0.000186	-0.170870	0.072552	0.170684	-0.243422	0.414106
56 C	0.001486	-0.142347	0.011112	0.143833	-0.153459	0.297292
57 C	0.000508	-0.077627	-0.020696	0.078135	-0.056931	0.135066
58 H	0.000027	0.185566	-0.004823	-0.185539	0.190389	-0.375928
59 C	0.000008	-0.074801	0.043612	0.074809	-0.118413	0.193222
60 H	-0.000187	0.182826	-0.001753	-0.183013	0.184579	-0.367592
61 C	0.000070	-0.122688	0.326728	0.122758	-0.449416	0.572174
62 H	-0.000002	0.178012	-0.018920	-0.178014	0.196932	-0.374946
63 Cl	0.000155	-0.001910	-0.000460	0.002065	-0.001450	0.003515
64 Cl	0.000213	-0.009747	-0.000614	0.009960	-0.009133	0.019093

Table 3. Mulliken atomic charges, Fukui indices and dual descriptor of CTZ using DFT at B3LYP/6-31G (d)

Atoms	$q_k(N+1)$	$q_k(N)$	$q_k(N-1)$	f_k^+	f_k^-	$\Delta f_k(r)$
1 C	0.046440	-0.158170	0.068410	0.204610	-0.226580	0.431190
2 C	-0.005050	-0.126960	-0.022550	0.121910	-0.104410	0.226320
3 C	0.013480	0.097180	0.075040	-0.083700	0.022140	-0.105840
4 C	0.037600	-0.298270	0.104440	0.335870	-0.402710	0.738580
5 C	-0.000652	-0.113810	-0.036950	0.113158	-0.076860	0.190018
6 C	0.006880	-0.128870	0.092370	0.135750	-0.221240	0.356990
7 H	-0.001930	0.132150	-0.004210	-0.134080	0.136360	-0.270440
8 H	-0.000268	0.147160	0.001030	-0.147428	0.146130	-0.293558
9 H	-0.001570	0.181010	-0.005580	-0.182580	0.186590	-0.369170
10 H	-0.000161	0.132660	0.001600	-0.132821	0.131060	-0.263881
11 H	-0.000433	0.132510	-0.005650	-0.132943	0.138160	-0.271103
12 C	-0.013480	0.000974	0.021260	-0.014454	-0.020286	0.005832

Atoms	$q_k(N+1)$	$q_k(N)$	$q_k(N-1)$	f_k^+	f_k^-	$\Delta f_k(r)$
13 C	0.087180	0.105740	0.073460	-0.018560	0.032280	-0.050840
14 C	0.063790	-0.206790	0.119920	0.270580	-0.326710	0.597290
15 C	-0.028510	-0.134390	-0.027780	0.105880	-0.106610	0.212490
16 C	-0.026250	-0.135870	-0.039430	0.109620	-0.096440	0.206060
17 H	-0.002830	0.163300	-0.006960	-0.166130	0.170260	-0.336390
18 C	0.057860	-0.151460	0.081050	0.209320	-0.232510	0.441830
19 H	0.000652	0.155780	0.000405	-0.155128	0.155375	-0.310503
20 C	0.060760	-0.128470	0.097290	0.189230	-0.225760	0.414990
21 H	0.000713	0.138450	0.001300	-0.137737	0.137150	-0.274887
22 H	-0.002480	0.138570	-0.005080	-0.141050	0.143650	-0.284700
23 H	-0.002680	0.135370	-0.005970	-0.138050	0.141340	-0.279390
24 C	0.064510	0.115430	0.089320	-0.050920	0.026110	-0.077030
25 C	0.011720	-0.207190	0.164270	0.218910	-0.371460	0.590370
26 C	-0.000983	-0.097570	-0.045950	0.096587	-0.051620	0.148207
27 C	-0.008010	-0.126560	-0.033160	0.118550	-0.093400	0.211950
28 C	0.001500	-0.183930	0.144170	0.185430	-0.328100	0.513530
29 H	-0.001550	0.199950	0.001340	-0.201500	0.198610	-0.400110
30 C	0.041020	-0.122150	0.082090	0.163170	-0.204240	0.367410
31 H	0.000200	0.154280	0.000956	-0.154080	0.153324	-0.307404
32 H	-0.000142	0.146160	-0.008480	-0.146302	0.154640	-0.300942
33 H	-0.001700	0.143920	-0.005480	-0.145620	0.149400	-0.295020
34 Cl	0.011890	0.089640	0.004560	-0.077750	0.085080	-0.162830
35 N	0.008430	-0.420140	0.006860	0.428570	-0.427000	0.855570
36 C	0.229250	0.127910	0.006150	0.101340	0.121760	-0.020420
37 C	0.208730	0.020520	0.002090	0.188210	0.018430	0.169780
38 H	0.230390	-0.025840	0.000542	0.256230	-0.026382	0.282612
39 C	-0.010740	0.199150	-0.000502	-0.209890	0.199652	-0.409542
40 H	-0.008880	0.175420	0.001480	-0.184300	0.173940	-0.358240
41 H	-0.011170	0.150640	0.000544	-0.161810	0.150096	-0.311906
42 N	-0.053520	-0.417440	0.011800	0.363920	-0.429240	0.793160

Table 4. Mulliken atomic charges, Fukui indices and dual descriptor of TBZ using DFT at B3LYP/6-31G (d)

Atoms	$q_k(N+1)$	$q_k(N)$	$q_k(N-1)$	f_k^+	f_k^-	$\Delta f_k(r)$
1 C	0.296933	-0.148547	0.084021	0.445480	-0.232568	0.678048
2 C	-0.092226	-0.173826	0.063758	0.081600	-0.237584	0.319184
3 C	0.167686	0.357305	-0.018143	-0.189619	0.375448	-0.565067
4 C	0.135371	0.237262	-0.015418	-0.101891	0.252680	-0.354571
5 C	0.071703	-0.182972	0.129682	0.254675	-0.312654	0.567329
6 C	-0.020661	-0.142239	-0.037296	0.121578	-0.104943	0.226521
7 H	-0.013039	0.127719	-0.005038	-0.140758	0.132757	-0.273515
8 H	0.002954	0.126107	-0.003950	-0.123153	0.130057	-0.253210
9 H	-0.003990	0.143244	-0.006694	-0.147234	0.149938	-0.297172
10 H	-0.000103	0.127025	0.001170	-0.127128	0.125855	-0.252983
11 C	0.140353	0.487276	0.137379	-0.346923	0.349897	-0.696820
12 N	-0.039596	-0.765538	0.024209	0.725942	-0.789747	1.515689
13 H	0.000752	0.327890	0.000615	-0.327138	0.327275	-0.654413
14 N	0.086376	-0.532410	0.056077	0.618786	-0.588487	1.207273
15 C	0.030498	0.265186	0.019340	-0.234688	0.245846	-0.480534
16 C	0.163800	-0.400414	0.433023	0.564214	-0.833437	1.397651
17 C	0.040562	-0.117466	0.101133	0.158028	-0.218599	0.376627
18 N	-0.012013	-0.361397	-0.036472	0.349384	-0.324925	0.674309
19 H	-0.007933	0.175801	-0.024772	-0.183734	0.200573	-0.384307
20 H	-0.002257	0.191367	-0.006685	-0.193624	0.198052	-0.391676
21 S	0.054829	0.258626	0.104061	-0.203797	0.154565	-0.358362

Table 5. Mulliken atomic charges, Fukui indices and dual descriptor of TCZ using DFT at B3LYP/6-31G (d)

Atoms	$q_k(N+1)$	$q_k(N)$	$q_k(N-1)$	f_k^+	f_k^-	$\Delta f_k(r)$
1 C	0.183028	-0.36171	0.104877	0.544738	-0.466587	1.011325
2 C	-0.007783	-0.09464	-0.010105	0.086857	-0.084535	0.171392
3 C	0.052624	0.1613	0.026748	-0.108676	0.134552	-0.243228
4 C	0.170657	-0.35665	0.163793	0.527307	-0.520443	1.04775
5 S	-0.030862	0.30463	0.045116	-0.335492	0.259514	-0.595006
6 H	-0.008462	0.18412	-0.006456	-0.192582	0.190576	-0.383158
7 H	-0.000251	0.16843	0.000522	-0.168681	0.167908	-0.336589
8 Cl	0.068457	0.02562	0.001388	0.042837	0.024232	0.018605
9 C	-0.003396	-0.08773	0.007305	0.084334	-0.095035	0.179369
10 H	0.001878	0.14918	-0.0004	-0.147302	0.14958	-0.296882
11 H	0.005323	0.15619	0.002794	-0.150867	0.153396	-0.304263
12 O	0.006846	-0.48606	0.008154	0.492906	-0.494214	0.98712
13 C	-0.000427	0.08186	0.018161	-0.082287	0.063699	-0.145986
14 H	-0.000135	0.13564	-0.000595	-0.135775	0.136235	-0.27201
15 C	0.00522	-0.19138	0.00977	0.1966	-0.20115	0.39775
16 H	0.000942	0.18267	0.004681	-0.181728	0.177989	-0.359717
17 H	-0.000027	0.19096	0.000072	-0.190987	0.190888	-0.381875
18 N	-0.01496	-0.37081	-0.000212	0.35585	-0.370598	0.726448
19 C	0.192777	0.18863	0.000446	0.004147	0.188184	-0.184037
20 C	0.17348	0.00902	0.000568	0.16446	0.008452	0.156008
21 H	-0.009397	0.1511	0.000105	-0.160497	0.150995	-0.311492
22 C	0.176096	-0.04164	0.000428	0.217736	-0.042068	0.259804
23 H	-0.007427	0.15652	-0.000181	-0.163947	0.156701	-0.320648
24 H	-0.008563	0.13547	-0.000031	-0.144033	0.135501	-0.279534
25 N	-0.051831	-0.43455	0.000043	0.382719	-0.434593	0.817312
26 C	0.043082	0.15571	0.220647	-0.112628	-0.064937	-0.047691
27 C	-0.003144	-0.1777	-0.01918	0.174556	-0.15852	0.333076
28 C	0.008378	-0.13388	0.150551	0.142258	-0.284431	0.426689
29 C	0.010219	-0.12074	0.089913	0.130959	-0.210653	0.341612
30 H	-0.000139	0.15942	-0.000357	-0.159559	0.159777	-0.319336
31 C	-0.003627	-0.12687	-0.076773	0.123243	-0.050097	0.17334
32 C	0.025963	-0.06292	0.258173	0.088883	-0.321093	0.409976
33 H	-0.000496	0.16861	-0.006203	-0.169106	0.174813	-0.343919
34 H	0.000035	0.18155	0.002656	-0.181515	0.178894	-0.360409
35 Cl	0.006352	-3.10E-05	0.001145	0.006383	-0.001176	0.007559
36 Cl	0.01957	6.69E-04	0.002438	0.018901	-0.001769	0.02067

The probable sites for nucleophilic attacks are the sites for which the values of the Fukui index f_k^+ and the dual descriptor are the highest. As for the electrophilic attack sites, they are identified by the highest value of the Fukui index f_k^- and by the lowest value of the dual descriptor $\Delta f_k(r)$. In case of ambiguity the atom

with the largest value and the lowest value of $\Delta f_k(r)$ for the same compound are respectively the probable sites for nucleophilic and electrophilic attacks. Thus in view of the above and after analysis Tables 2, 3, 4 and 5, the different sites of reactivity of the studied molecules are recorded in Table 6.

Table 6. Recap of the different reactivity atoms

Molecules	Probable sites for nucleophilic attacks	Probable sites for electrophilic attacks
KTZ	N(20)	C(1)
CTZ	N(35)	C(39)
TBZ	N(12)	C(11)
TCZ	C(4)	S(5)

It appears that the studied inhibitors reactivity strongly depends on N,S heteroatoms and C carbon atom. However the probable sites for nucleophilic attacks are dominated by nitrogen atoms (N). In addition these sites associated with the LUMO orbital could receive electrons that would come from the metal. Regarding the probable sites for electrophilic attacks, they are dominated by carbon atoms (C) with the presence of a sulfur atom (S). These sites are likely to donate electrons to the metal. Therefore, these electrophilic attack sites are associated with the HOMO. The donor-acceptor properties that these molecules possess give them a good ability to protect copper against corrosion in nitric acid solution.

The inhibitor molecules are protonated in nitric acid medium. Thiabendazole is protonated according to the chemical in following equation:

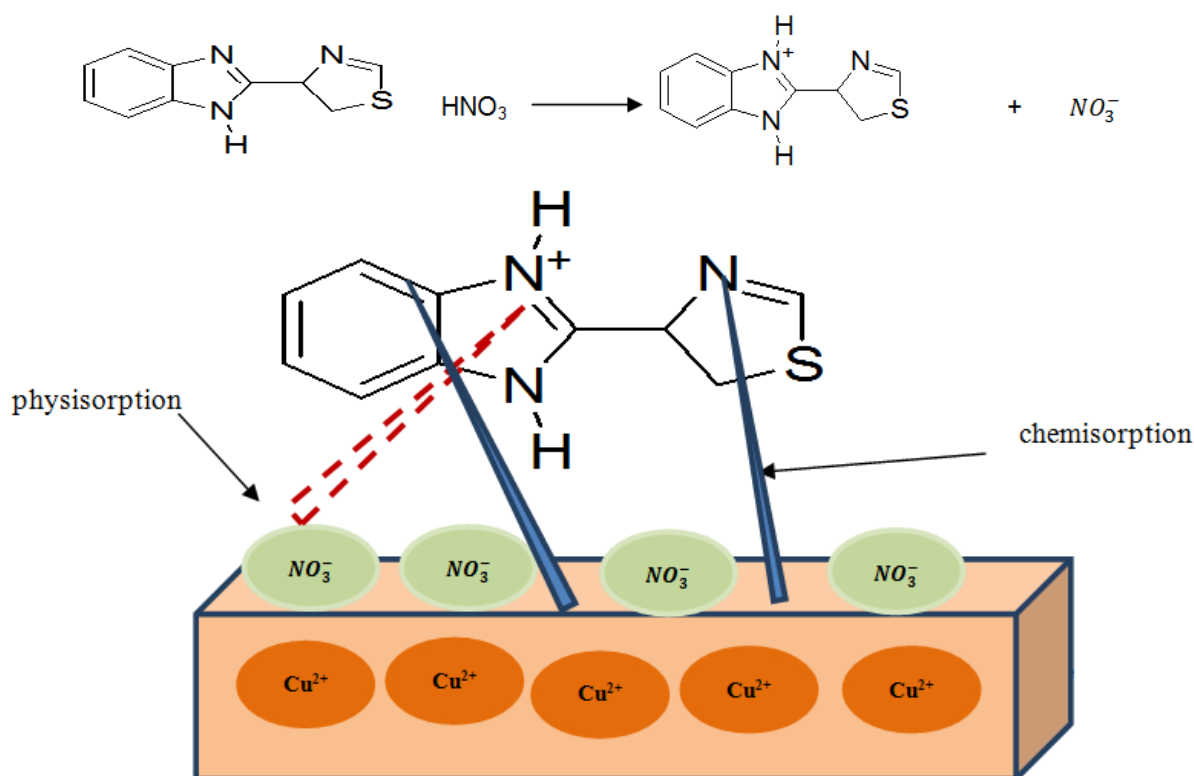


Fig. 4. Pictorial representation of Thiabendazole adsorption on copper surface in 1.0 M HNO_3

The inhibitor molecule protonated formed in the solution will permit the compound to adsorb on the copper surface negatively charged by NO_3^- ions. Thanks to the charge carried by the proton, the latter, interacting with the negative charge of the nitrate ions, gives rise to electrostatic interactions that promote physisorption. The free electron pairs of the heteroatoms belong to each compound studied, as well as the π electrons of the aromatic rings which help the molecule to adsorb on copper surface. This adsorption is facilitated by the presence of the unfilled d-orbitals gives importance to the donor-acceptor interactions between the molecule and the metal surface favoring the chemisorption. Indeed this chemisorption is due to the heteroatoms and

electrons present in the structures of the studied compounds will certainly provide enough electrons to the vacant 3d orbitals of the metal for the formation of a stable coordination bond.

Fig. 4 explains the mechanism of adsorption.

4. CONCLUSION

Quantum chemical studies justified by DFT calculations revealed that the inhibitory power of KTZ, CTZ, TBZ and TCZ is promoted by their electron donor-acceptor ability. These inhibition properties could strengthen the copper surface by reducing its degradation. The inhibition capacity of the four studied inhibitors related to

highest occupied molecular orbital energy (E_{HOMO}), lowest unoccupied molecular orbital energy (E_{LUMO}), the energy gap (ΔE) and the fraction of transferred electrons (ΔN). The relative ability of the studied molecules to inhibit copper corrosion is found to be dependent on the relative ability of the compounds to donate electrons to the metal. It was found that TBZ could have the best inhibitory performance in copper corrosion in the studied solution. The total energy values of the studied compounds predict that the electronic exchanges between them and copper are favorable. Furthermore, the values of Fukui indices and dual descriptor led to accurate predictions of the positions for electrophilic and nucleophilic attack. These positions also estimated the importance of nitrogen, carbon and sulfur atoms in the local reactivity. In addition, these results could facilitate the design of new corrosion inhibitors with the same chemical functions as the studied compounds that can be used in the protection of metals.

COMPETING INTERESTS

Authors have declared that no competing interests exist.

REFERENCES

1. Finšgar M, Jackson J. Application of corrosion inhibitors for steels in acidic media for the oil and gas industry: A review. *Corrosion Science*. 2014;86:17–41.
2. Niamien PM, Essy F K, Trokourey A, Yapi A, Aka H.K. and Diabate D. Correlation between the molecular structure and the inhibiting effect of some benzimidazole derivatives. *Materials Chemistry and Physics*. 2012;136(1):59-65.
3. Sílvia de Souza F., Giacomelli C. , Reinaldo Simões Gonçalves R.S. , Almir Spinelli A. Adsorption behavior of caffeine as a green corrosion inhibitor for copper. *Materials Science and Engineering C*. 2012;32:2436–244.
4. Tigori MA, Kouyaté A, Kouakou V, Niamien PM, Trokourey A. Inhibition performance of some sulfonylurea on copper corrosion in nitric acid solution evaluated theoretically by DFT calculations. *Open Journal of Physical Chemistry*. 2020;10(3):139-157.
5. Tigori MA, Kouyaté A, Kouakou V, Niamien PM, Trokourey A. Computational approach for predicting the adsorption properties and inhibition of some antiretroviral drugs on copper corrosion in HNO₃. *European Journal of Chemistry*. 2020;11(3):235-244.
6. Yadav M, Debasis B, Sumit K, Rajesh RS. Experimental and Quantum Chemical Studies on the Corrosion Inhibition Performance of Benzimidazole Derivatives for Mild Steel in HCl. *Industrial & Engineering Chemistry Research*. 2013;52(19):6318-6328.
7. Hassane Lgaz, Ill-Min Chung, Mustafa R. Albayati, Abdelkarim Chaouiki, Rachid Salghi, Shaaban K. Mohamed. Improved corrosion resistance of mild steel in acidic solution by hydrazone derivatives: An experimental and computational study. *Arabian Journal of Chemistry*. 2020;13(1):2934-2954.
8. Khattabi M, Benhiba F, Tabti S, Djedouani A, El Assyry A, Touzani R, Warad I, Oudda H, Zarrouk A. Performance and computational studies of two soluble pyran derivatives as corrosion inhibitors for mild steel in HCl. *Journal of Molecular Structure*. 2019;1196: 231-244.
9. Eddy NO, Momoh-Yahaya H, Oguzie EE. Theoretical and experimental studies on the corrosion inhibition potentials of some purines for aluminium in 0.1 M HCl. *Journal of Advanced Research*. 2015;6:203-217.
10. Tecuapa-Flores ED, Turcio-Ortega D, Guadalupe Hernandez J, Huerta-Aguilar CA, Thangarasu P. The role of keto group in cyclic ligand 1,4,8,11-tetraazacyclotetradecane-5,7-dione as strong corrosion inhibitor for carbon steel surface: Experimental and theoretical studies. *Journal of Molecular Structure*. 2019;1189:131-145.
11. Thomas LH. The calculation of atomic fields. *Mathematical Proceedings of the Cambridge Philosophical Society*. 1927;23(5):542–548.
12. Fermi E. Un metodo statistico per la determinazione di alcune proprietà dell'atome, *Rendiconti Accademia Nazionale dei Lincei*. 1927;6:602-607.
13. Qiang Y, Zhang S, Yan S, Zou X, Chen S. Three indazole derivatives as corrosion inhibitors of copper in a neutral chloride solution. *Corrosion Science*. 2017;126:295–304.
14. Ahamad I, Prasad R, Quraishi MA. Experimental and theoretical investigations of adsorption of fexofenadine at mild steel/hydrochloric acid interface as

- corrosion inhibitor. *Journal of Solid State Electrochemistry*. 2010;14:2095–2105.
15. David M. Bastidas, Adsorption of benzotriazole on copper surfaces in a hydrochloric acid solution, surface and interface analysis. 2006;38(7):1146-1152.
 16. Singh AK, Mohapatra S, Pani B. Corrosion inhibition effect of aloe vera gel: Gravimetric and electrochemical study. *Journal of Industrial and Engineering Chemistry*. 2016;25:288-297.
 17. Deyab MA. Egyptian Licorice extract as a green corrosion inhibitor for copper in hydrochloric acid solution. *Journal of Industrial and Engineering Chemistry*. 2015;25:384-389.
 18. Eddy NO, Ebenso EE, Ibok UJ. Adsorption, synergistic inhibitive effect and quantum chemical studies of ampicillin (AMP) and halides for the corrosion of mild steel in H₂SO₄. *Journal of Applied Electrochemistry*. 2009;40(1):445-456.
 19. Yeo M, Niamien PM, Ehui Bernadette Avo BEB, Albert Trokourey A. Thiamine Hydrochloride as a Potential Inhibitor for Aluminium Corrosion in 1.0 M HCl: Mass Loss and DFT Studies. *Journal of Computational Methods in Molecular Design*. 2018;8(1):13-25.
 20. Obot IB, Obi-Egbedi NO. Fluconazole as an inhibitor for aluminium corrosion in 0.1 M HCl, *Colloids and Surfaces A: Physicochemical and Engineering Aspects*. 2008;330(2-3): 207-212.
 21. Singh AK, Quraishi MA. Effect of Cefazolin on the Corrosion of Mild Steel in HCl Solution. *Corrosion Science*. 2009;52:152-160.
 22. Alagarsamy V, Solomon VR, Dhanabal K. Synthesis and pharmacological evaluation of some 3-phenyl-2-substituted-3H-quinazolin-4-one as analgesic, anti-inflammatory agents. *Bioorganic & Medicinal Chemistry*. 2007;15:235–241.
 23. Frisch MJ, Trucks GW, Schlegel HB, Scuseria GE, Robb, MA, Cheeseman JR, et al. *Gaussian 09*. Gaussian, Inc., Wallingford, CT; 2009.
 24. Yang W, Parr RG. Hardness, softness, and the Fukui function in the electronic theory of metals and catalysis. *Proceeding of the National Academy of Sciences*. 1985;82(20):6723-6726.
 25. N. Lopez, Illas F. Ab initio modeling of the metal-support interface: the interaction of Ni, Pd, and Pt on MgO(100), *Journal of Physical Chemistry B*. 1998;102(8):1430–1436.
 26. Koopmans T. About the Assignment of Wave Functions and Eigenvalues to the Individual Electrons of Atoms. Über die Zuordnung von Wellenfunktionen und Eigenwerten zu den Einzelnen Elektronen eines Atoms. *Physica*. 1934;1:104-113.
 27. Parr RG, Yang W. Absolute hardness: Comparison parameter to absolute electronegativity. *Journal of the American Chemical Society*. 1983;105:7512-7516.
 28. Yang W, Parr RG. Absolute electronegativity and hardness correlated with molecular orbital theory. *Proceeding of the National Academy of Sciences*. 1986;83:8440-8441.
 29. Parr RG, Szentpaly L, Liu S. Electrophilicity Index. *Journal of the American Chemical Society*. 1999;121:1922-1924.
 30. Pearson RG. Absolute Electronegativity and hardness: Application to inorganic chemistry. *Inorganic Chemistry*. 1988;27:734-740.
 31. Michaelson HB. The work function of the elements and its periodicity. *Journal of Applied Physics*. 1977;48:4729-4733.
 32. Dewar MJS, Zoebisch EG, Healy EF, Stewart JP. Development and use of quantum mechanical molecular models, 76, AM1: A new general purpose quantum mechanical molecular model. *Journal of the American Chemical Society*. 1985;107:3902-3909.
 33. Martínez-Araya J.I., Why the dual descriptor is a more accurate local reactivity descriptor than Fukui functions? *Journal of Mathematical Chemistry*. 2015;53: 451-465.
 34. Morell C, Grand A, Toro Labbe A. New dual descriptor for chemical reactivity. *Journal of Physical Chemistry. A*. 2004;109(1):205-212.
 35. Musa AY, Kadhum AAH, Mohamad AB, Rahoma AAB, Mesmari H. Electrochemical and quantum chemical calculations on 4,4-dimethylloxazolidine-2-thione as inhibitor for mild steel corrosion in hydrochloric acid. *Journal of Molecular Structure*. 2010; 969(1–3): 233–237.
 36. Abdelqader EG, Abderrahim T, Karima C, Naoual M, Mohamed EIA, Rachid T, Belkheir H, Hassane L. The synergistic effect of chloride ion and 1,5-Diaminonaphthalene on the Corrosion inhibition of mild steel in 0.5 M Sulfuric

- Acid: Experimental and Theoretical Insights. Surfaces and Interfaces. 2018;13:168-177.
37. Ahamad I, Prasad R, Quraishi MA. Adsorption and inhibitive properties of some new Mannich bases of Isatin derivatives on corrosion of mild steel in acidic media. Corrosion Science. 2010;52(4):1472-1481.
 38. Loutfy H, Madkour S, Kaya Lei G, Cemal K. Quantum chemical calculations, molecular dynamic (MD) simulations and experimental studies of using some azo dyes as corrosion inhibitors for iron. Part 2: Bis-azo dye derivatives. Journal of Molecular Structure. 2018;1163:397-417.
 39. Singh A, Ansari KRA, Kumar A, Liu W, Songsong C, Liu Y. Electrochemical, surface and quantum chemical studies of novel imidazole derivatives as corrosion inhibitors for J55 steel in sweet corrosive environment. Journal of Alloys and Compounds. 2017;72:121-133.
 40. Reza Teimuri-Mofrad, Iraj Ahadzadeh, Mahdi Gholamhosseini-Nazari, Somayeh Esmati, Aziz Shahrissa. Synthesis of Betti base derivatives catalyzed by nano-CuO-ionic liquid and experimental and quantum chemical studies on corrosion inhibition performance of them. Research on Chemical Intermediates. 2018;44(4):2913-2927.
 41. Lukovits I, Kalman E, Zucchi F. Corrosion Inhibitors-correlation between electronic structure and efficiency. Corrosion. 2001;57:3-8.
 42. Nwankwo HU, Olasunkanmi LO, Ebenso EE. Experimental, quantum chemical and molecular dynamic simulations studies on the corrosion inhibition of mild steel by some carbazole derivatives. Scientific Report. 2017;7:2436-2446.
 43. Mohamed EF, Fouad B, Hafida A, Younes K, Abdellah G, Brahim L, Ismail W, Chandrabhan V, El-Sayed MS, Ebenso EE, Zarrouk A. Experimental and computational investigations on the anti-corrosive and adsorption behavior of 7-N,N'-dialkylaminomethyl-8-Hydroxyquinolines on C40E steel surface in acidic medium, Journal of Colloid and Interface Science. 2020;576:330-344.
 44. Hong J, Li X, Cao N, Wang F, Liu Y, Li Y. Schiff-base derivatives as corrosion inhibitors for carbon steel materials in acid media: quantum chemical calculations. Corrosion Engineering, Science and Technology. 2018;53:1:36-43.
 45. Kouakou V, Niamien PM, Yapo AJ, Trokourey A. Copper Corrosion Inhibition in 1M Nitric Acid: Adsorption and Inhibitive Action of Theophylline. Chemical Science Review and Letter. 2016;5(20):131-146.
 46. Lei Guo, Shan hong Zhu, Sheng tao Zhang, Qiao He, Weihua Li. Theoretical studies of three triazole derivatives as corrosion inhibitors for mild steel in Acidic medium, Corrosion Science. 2014;87:366-375.
 47. Lei Guo L, Kaya S, Obot IB, Zheng X, Qiang Y. Toward understanding the anticorrosive mechanism of some thiourea derivatives for carbon steel corrosion: A combined DFT and molecular dynamics investigation. Journal of Colloid and Interface Science. 2017;506:478-485.

© 2022 M'Bouillé et al.; This is an Open Access article distributed under the terms of the Creative Commons Attribution License (<http://creativecommons.org/licenses/by/4.0>), which permits unrestricted use, distribution, and reproduction in any medium, provided the original work is properly cited.

Peer-review history:
The peer review history for this paper can be accessed here:
<https://www.sdiarticle5.com/review-history/85376>